

512-37  
87/49

# **H<sup>∞</sup> CONTROL OF MAGNETIC BEARINGS TO ENSURE BOTH SYSTEM AND EXTERNAL PERIODIC DISTURBANCE ROBUSTNESS**

**Yuhong Jiang and R. B. Zmood**

**Department of Electrical Engineering  
Royal Melbourne Institute of Technology  
Melbourne Victoria 3000, Australia**

## **SUMMARY**

Both self-excited and forced disturbances often lead to severe rotor vibrations in a magnetic bearing systems with long slender shafts. This problem has been studied using the H<sup>∞</sup> method, and stability with good robustness can be achieved for the linearized model of a magnetic bearing when small transient disturbances are applied. In this paper, the H<sup>∞</sup> control method for self-excited and forced disturbances is first reviewed. It is then applied to the control of a magnetic bearing rotor system. In modelling the system, the shaft is first discretized into 18 finite elements and then three levels of condensation are applied. This leads to a system with three masses and three compliant elements which can be described by six state variable coordinates. Simulation of the resultant system design has been performed at speeds up to 10,000 rpm. Disturbances in terms of different initial displacements, initial impulses, and external periodic inputs have been imposed. The simulation results show that good stability can be achieved under these different transient disturbances using the proposed controller while at the same time reducing the sensitivity to external periodic disturbances.

## **1. INTRODUCTION**

Magnetic bearings, because of their absence of physical contact with the bearing journal are well suited for high speed rotating machines (ref. 1). Additional advantages of magnetic bearings are the absence of mechanical wear and the need for lubrication. A system of magnetic bearings with a long slender shaft can often have severe vibrations due to rotor unbalance or self excited instabilities; especially when the shaft rotates at high speed. In the case of forced vibrations, such as due to unbalanced mass, the shaft will deflect from its axis of rotation as a result of these forces. Self excited rotor instability will also lead to severe rotor vibrations. The control task is, therefore, to restore the bearing journals to the central axes of the magnetic bearings within a short period of time after a transient disturbance, to minimise rotor vibration, and to exhibit

low sensitivity to external periodic disturbances. Thus the design of a controller for a magnetic bearing system poses a significant challenge. While PID controllers have been used extensively with magnetic bearings they do not easily satisfy the robust performance requirements of these systems. The application of LQG methods for bearing control also have their limitations as they are unable to adequately treat systems with plant uncertainty (ref. 2). So  $H^\infty$  control design methods (refs. 3 and 5) have attracted attention for designing the control systems of magnetic bearings, because  $H^\infty$  control theory includes frequency shaping techniques as used for conventional PID controllers as well as the optimisation methods used in modern LQG control design methods.

The present work concerns the application of the  $H^\infty$  control method to a magnetic bearing system as shown in Figure 1. The beam is supported horizontally by two magnetic bearings. The rotor is attached to the shaft midway between the two bearings. In applying  $H^\infty$  control, the system is considered to be a mixed sensitivity control problem, where the weighting functions are selected to assure a robust controller design. An algorithm for arriving at suitable weighting functions using the MATLAB software package for the controller design, is described and is applied to the above system. The designed system has been simulated for speeds up to 10,000 rpm. The results show the proposed magnetic bearing controller using this design method works well when the bearing system is subjected to various transient disturbances while at the same time it reduces the sensitivity of the system to external periodic disturbances.

## 2. MATHEMATICAL MODEL OF THE MAGNETIC BEARING SYSTEM

The magnetic bearing suspension system being considered has a flexible shaft as shown in Fig. 1. The shaft is supported at its left and right ends by the magnetic bearings

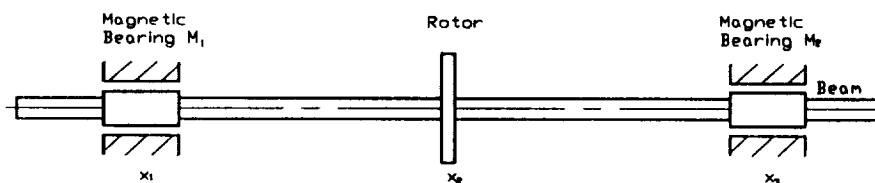


Figure 1. The rotor of the system.

$M_1$  and  $M_2$  with the rotor being positioned on the shaft midway between the two magnetic bearings. The displacements of the bearing journals are defined to be  $x_1$ , and  $x_2$ . The flexible shaft in this study is assumed to have a length  $L=600$  mm and a diameter  $D=10$  mm. In this system the bearing forces are generated by electro-magnet coils and the shaft position is detected by a displacement sensor. The sensor signals are fed through the controllers in to the power amplifiers which finally supply the excitation currents to the electro-magnet coils.

In the system model, the rotor flywheel structure was divided into 18 elements. The finite element method was used to calculate the mass and stiffness of the shaft. Three levels of condensation were applied to the 18 finite elements which led to a mathematical model of the shaft having 6 coordinates  $\{x\} = \{x_1, x_2, x_3, \dot{x}_1, \dot{x}_2, \dot{x}_3\}$  as shown in Fig. 1. The shaft mass and shaft stiffness were calculated to be

$$M_s = \begin{bmatrix} 0.6067 & -0.1465 & 0.0451 \\ -0.1465 & 2.2674 & -0.1465 \\ 0.0451 & -0.1465 & 0.6067 \end{bmatrix} \text{ and } K_s = \begin{bmatrix} 0.0454 & -0.0943 & 0.0472 \\ -0.0943 & 0.1943 & -0.0942 \\ 0.0472 & -0.0942 & 0.0466 \end{bmatrix}$$

respectively. The equations of motion for the simulation of the magnetic bearing system are given in Appendix I.

For the simulations, it is necessary to simulate the system dynamics using a set of first order differential equations. In this study, the magnetic bearing system is modelled using the state-space model of the continuous-time, equation (1)

$$\begin{aligned} \dot{x}_g &= A_g x_g + B_g u_g \\ y_g &= C_g x_g \end{aligned} \quad (1)$$

where  $\{x_g\} = \{x_1, x_2, x_3, \dot{x}_1, \dot{x}_2, \dot{x}_3\}$  are the displacements and velocities of the flywheel and shaft, and  $u_g = \{u_1, u_2, u_3\}$  are the output currents of the power amplifiers. The coefficient matrices for  $A_g, B_g, C_g$  are

$$A_g = \begin{bmatrix} 0_{3 \times 3} & I_{3 \times 3} \\ -M_s^{-1}(K_s + K_x) & 0_{3 \times 3} \end{bmatrix} \quad B_g = \begin{bmatrix} 0_{3 \times 3} \\ M_s^{-1}K_i \end{bmatrix}$$

$$C_g = \begin{bmatrix} 1 & 0 & 0 & 0 & 0 & 0 \\ 0 & 1 & 0 & 0 & 0 & 0 \\ 0 & 0 & 1 & 0 & 0 & 0 \end{bmatrix}$$

From the above parameter matrices, the matrices  $A_g$  and  $B_g$  can be shown to be

$$A_g = \begin{bmatrix} 0 & 0 & 0 & 1 & 0 & 0 \\ 0 & 0 & 0 & 0 & 1 & 0 \\ 0 & 0 & 0 & 0 & 0 & 1 \\ -0.095 & 0.179 & -0.06 & 0 & 0 & 0 \\ 0.028 & -0.033 & .029 & 0 & 0 & 0 \\ -0.064 & 0.172 & -0.10 & 0 & 0 & 0 \end{bmatrix} \quad B_g = \begin{bmatrix} 0 & 0 & 0 \\ 0 & 0 & 0 \\ 0 & 0 & 0 \\ -0.9299 & 0.0565 & 0.0555 \\ -0.0565 & -0.251 & -0.0565 \\ 0.0555 & -0.056 & -0.9299 \end{bmatrix}$$

with  $(A_g, B_g)$  being controllable, and  $(A_g, C_g)$  being observable. The system transfer function is  $G(s) = C_g(sI - A_g)^{-1} B_g$ .

If external periodic disturbances are applied to the magnetic bearing system, the system equations of motion are shown in Appendix II. In this case the state-space model for the system is

$$\begin{aligned}\dot{x}_g &= A_g x_g + B_g u_g + B_{1g} F_d \\ y_g &= C_g x_g\end{aligned}\quad (2)$$

where  $B_{1g} = \begin{bmatrix} 0_{3 \times 3} \\ M_s^{-1} \end{bmatrix}$

Plant uncertainty, air gap growth with high speed shaft rotation, shaft parameter estimation errors and the effect of eddy-currents in the electromagnets will all affect the coefficient matrices in the above equations, and thus will influence the magnetic bearing control system stability and periodic disturbance robustness.

### 3. CONTROLLER DESIGN

$H^\infty$  optimal control design offers a robust performance by addressing disturbances and plant uncertainty. The  $H^\infty$  optimal controller takes into consideration the plant uncertainty bandwidth, and disturbance attenuation, and achieves the best system performance (ref. 4). The design will be carried out using the computer package ROBUST CONTROL TOOLBOX with MATLAB (ref. 6).

#### 3.1 Mixed-Sensitivity Robust Control

The augmented plant and controller diagram is shown in Fig. 2. The transfer function  $S$  from  $u_1$  to  $e$  is termed the sensitivity function and the transfer function  $T$  from  $u_2$  to  $y_2$  is called the complementary function, also  $F$  is the controller for the system. The functions  $S$  and  $T$  are defined as

$$S = (I + GF)^{-1} \quad T = I - S = GF(I + GF)^{-1}$$

In the case of the mixed sensitivity problem, the cost function is shown to be

$$\left\| T_{y_1 u_1} \right\| = \left\| \begin{bmatrix} W_1(s)S(s) \\ W_3(s)T(s) \end{bmatrix} \right\|_\infty < 1$$

where  $\|\cdot\|_\infty$  denotes the  $H$ -infinity norm.  $W_3(s)$  is the frequency weighting function used for robustness stabilisation at high frequencies and  $W_1(s)$  is used for sensitivity reduction at low frequencies. Both of these matrices need to be selected according to the

requirements of system performance, plant uncertainty bandwidth, and the input and output disturbances of the plant. The augmented plant  $P(s)$  of the plant  $G(s)$  with the weighting functions  $W_1(s)$  and  $W_3(s)$  is shown in Fig. 2, where  $u_1$  is the disturbance input at the input of the plant,  $u$  is the control input vector,  $y_{11}$  and  $y_{12}$  are the closed-loop system output vectors, and  $y_2$  is the measured output vector. The state vector  $x$  of the plant  $G(s)$  is not shown on this diagram.

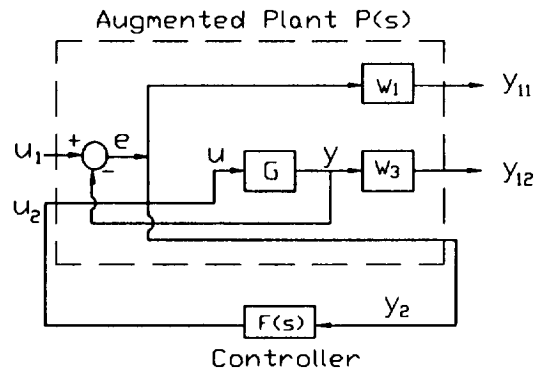


Figure 2. Closed-loop control diagram.

### 3.2 $H^\infty$ Method Design

The magnetic bearing system is subject to different types of disturbances as discussed above. For the disturbances which act on the plant at low frequencies, the performance can be calculated using the sensitivity function  $S$ . This can be specified using the performance weighting function  $W_1(s)$  so that

$$\|W_1(s)S(s)\|_\infty < 1$$

$W_1(s)$  is taken as a low pass filter in order to choose the bandwidth of the closed loop and to reduce the output deviation at low frequencies by introducing a quasi-integral action in the controller. A weighting function  $W_1(s)$  satisfying these requirements is given by

$$W_1(s) = \frac{\gamma(s + 10^4)}{10^2(s + 100)} [1 \quad 1 \quad 1]^T$$

where  $\gamma$  is an adjustable parameter which can be set by the designer. Initially it is useful to take  $\gamma=1$  and then to increase it according to the system performance requirements. It has been found that  $\gamma=2.86$  is the most appropriate value for this design.

As the magnetic bearing system has air gap growth at high speeds this causes the bearing characteristics to change. To make the stability of the magnetic bearings more robust at high frequencies, the stability robustness can be specified using the uncertainty weighting function  $W_3(s)$  so that

$$\|W_3(s)T(s)\|_{\infty} \leq 1$$

The weighting function  $W_3(s)$  is taken as a high pass filter in order to reduce the control effect at high frequencies. An uncertainty weighting function  $W_3(s)$  satisfying these needs is

$$W_3(s) = \frac{s^2}{10^5} [1 \ 1 \ 1]^T$$

The  $H^{\infty}$  optimal controller design can be analysed using the Robust-Control Toolbox in MATLAB. With the weighting functions  $W_1(s)$  and  $W_3(s)$ , an augmented plant can be formed which is shown in Fig. 3, and then we can use MATLAB to calculate the state-space realisation of the augmented plant as follows

$$\begin{aligned} \dot{x} &= Ax + B_1 u_1 + B_2 u_2 \\ y_1 &= C_2 x + D_{11} u_1 + D_{12} u_2 \\ y_2 &= C_2 x + D_{21} u_1 + D_{22} u_2 \end{aligned}$$

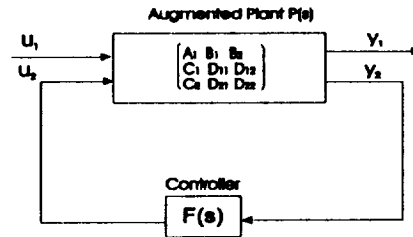


Figure 3.  $H^{\infty}$  feedback diagram.

External periodic disturbances, different initial condition disturbances, and transient disturbances will be applied to the input  $u_1$  after the controller has been obtained.

### 3.3. The Closed-Loop Transfer Function $T(s)$

The model reduction algorithm (ref. 6) in the Robust Control Toolbox in MATLAB was applied to the  $H^{\infty}$  feedback system to find a reduced 6 state variable model that satisfied the "robustness criterion". Fig. 3 shows a standard  $H^{\infty}$  optimal control system, which has an augmented plant  $P(s)$  and a feedback controller  $F(s)$ . The stabilising feedback control law  $u_2 = F(s)y_2(s)$  was found so that the  $H^{\infty}$  norm of the closed-loop transfer function matrix

$$T_{y,u_1} = P_{11}(s) + P_{12}(s)(1 - F(s)P_{22}(s))^{-1} F(s)P_{21}(s)$$

is small. The  $H^{\infty}$  control problem thus reduces to finding  $F(s)$  so as to satisfy the inequality  $\|T_{y,u_1}\| < 1$ . The closed-loop frequency responses of the bearing system represented by the singular value of  $T_{y,u_1}$  is shown in Fig. 4. With the selected controller  $F(s)$ , the system has good performance for frequencies up to 1000 rad/sec, which corresponds to speeds of 10,000 rpm.

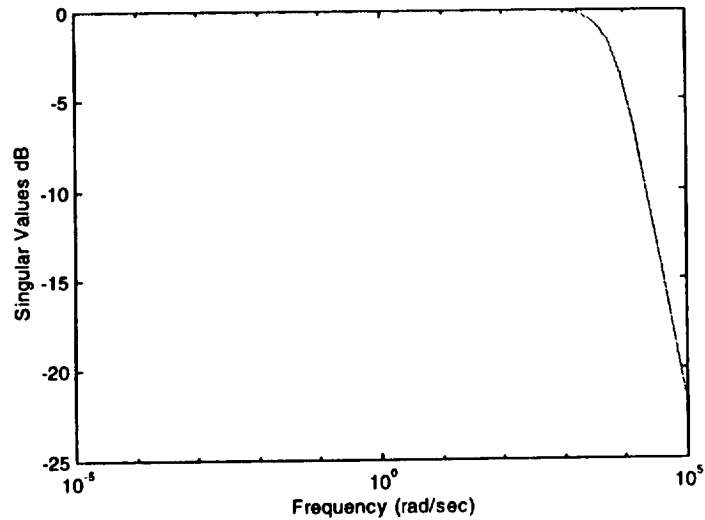


Figure 4. Closed-loop frequency response (Singular value of  $T_{y,u_1}$  ).

## 4. SIMULATION RESULTS

### 4.1 Simulation Results for Self-Excited Disturbances

In this section we evaluate the stability of the designed control system by studying the transient time response for impulse disturbances and non zero initial conditions. These disturbances have been applied to the augmented plant, and the simulated responses computed using the Robust-Control Toolbox in MATLAB, are shown in Figs. 5 and 6. From the simulation results for an impulse input, we can see that it takes 0.025 seconds to restore the shaft to its rest position while for non-zero initial conditions the settling time is approximately 0.02 seconds. From these time response plots it will also be noted that the performance of the bearing control is very well damped.

### 4.2 Simulation Results for External Periodic Disturbances

In this section we examine the operation of the  $H^\infty$  magnetic bearing control systems while the rotor experiences external periodic disturbances. A number of cases of periodic disturbances using unbalance eccentricities have been simulated as shown in Table 1.

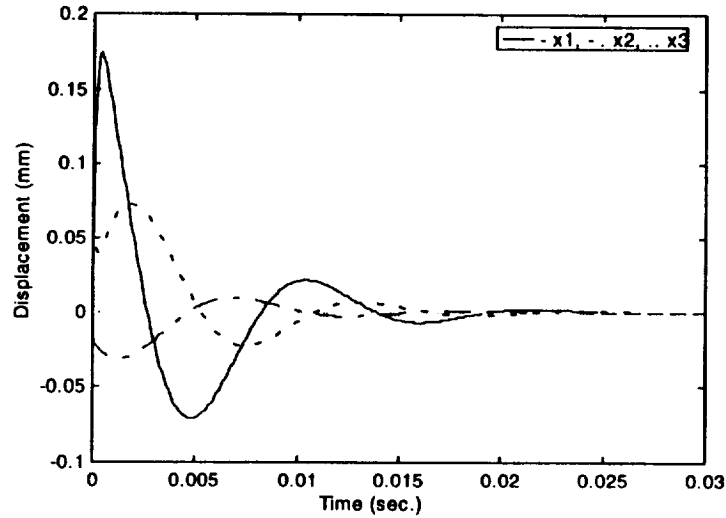


Figure 5. System response for impulse disturbance input.

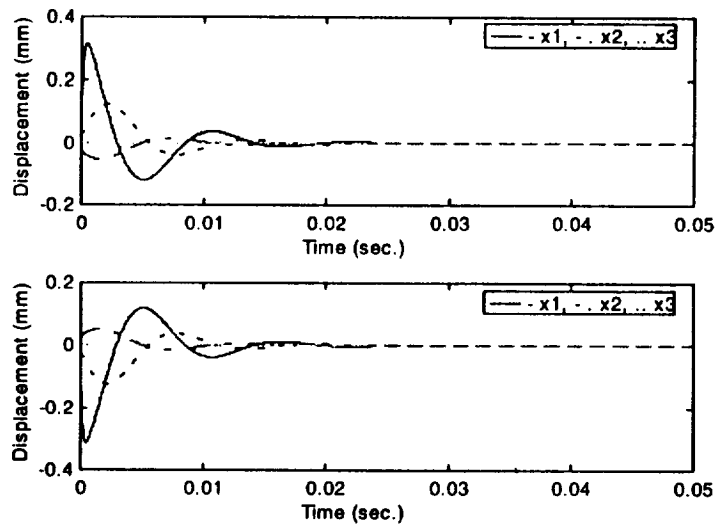


Figure 6. System response for different non-zero initial conditions.

In Fig. 7 we show the simulated results for case 1 only as the remaining cases are similar. It can be seen that for initial journal displacements of  $x_1 = -0.2$  mm and  $x_3 = +0.2$  mm, when rotating at speed of 10 and 20 rad/sec, it returns to its steady state condition in about 0.06 secs, so that it thereafter rotates about its geometric axis. However when rotating at speeds of 40 and 70 rad/sec it can be seen from Fig. 8 that the shaft begins to rotate about its principal inertial axis. The trade off between the sensitivity to transient and external periodic disturbances is determined by the choice of the performance weighting function  $W_f(s)$ .



Table 1.

Line	Unbalanced Eccentricity $\mu^T$ (mm)	Rotor mass (kg)	Speed Range $\omega$ (rad/sec)
1	$\mu^T = \{-0.009, -0.003, 0.005\}$	1.13	10,20,40,70
2	$\mu^T = \{-0.0009, -0.0003, .0005\}$	1.22	10,20,40,70
3	$\mu^T = \{-0.009, -0.003, 0.005\}$	1.16	10,20,40
4	$\mu^T = \{-0.0009, -0.0003, .0005\}$	1.52	10,20,40

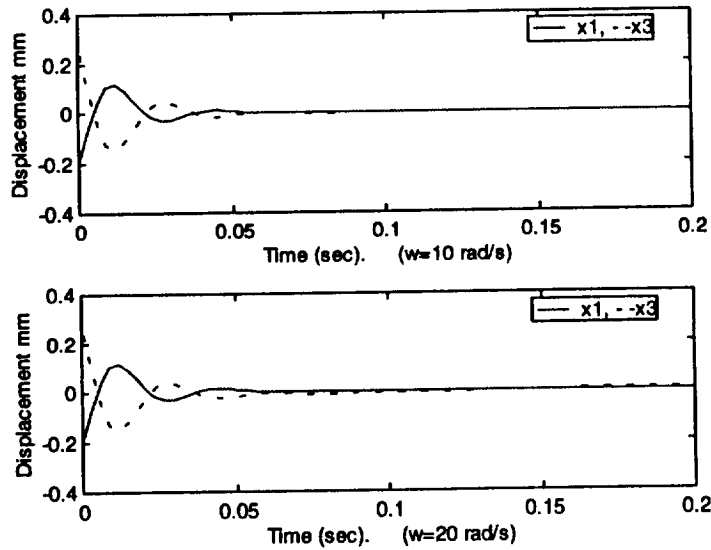


Figure 7. System responses with external periodic disturbance.

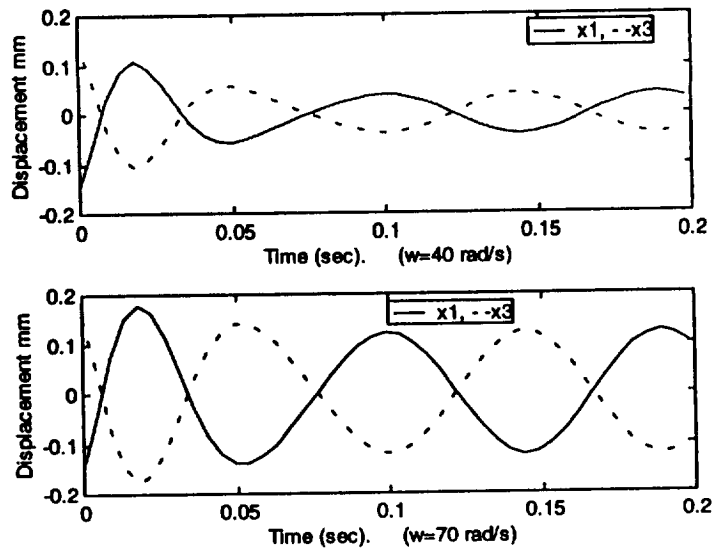


Figure 8. System responses with external periodic disturbance.

## 5. CONCLUSIONS

We have designed a  $H^\infty$  controller for a magnetic bearing system operating at speeds up to 10,000 rpm. In our study we have considered the plant to have an unstructured multiplicative uncertainty. In the case where the system has external periodic disturbances it can be seen that it has low sensitivity to these disturbances when operation is at speeds above 40 rad/sec. Also using the designed controller, the rotor can be suspended in a stable manner, and has good robustness to self-excited disturbances.

## ACKNOWLEDGMENTS

In this work the shaft mass and the shaft stiffness for the rotor system were calculated using the software package developed by Dr. J. Krodkiewski (ref. 7), from the Department of the Mechanical Engineering, University of Melbourne, Australia.

Part of this work was performed under the management of the Micromachine Centre as the Industrial Science and Technology Frontier Program, "Research and Development of Micromachine Technology", of MITI supported by New Energy and Industrial Technology Development Organisation.

## APPENDIX I: BEARING SYSTEM EQUATION OF MOTION - SELF DISTURBANCES

The equations of the motion of the magnetic bearing system can be shown to be

$$[M_s]\{\ddot{x}\} + ([K_s] + [K_x])\{x\} = K_i i$$

In this, the units of displacement  $x$ , mass of the shaft  $M_s$  and stiffness of the shaft  $K_s$  have the units of millimetre, kilogram, and newton/millimetre, respectively. The bearing actuator current sensitivity ( $K_i=23.06$  N/A), and the bearing actuator static stiffness ( $K_x=171.00$  N/mm), and  $i$  is the power amplifier output current.

## APPENDIX II: BEARING SYSTEM EQUATION OF MOTION - PERIODIC DISTURBANCES

The equations of the motion for the magnetic bearing system having external periodic disturbances can be shown to be

$$[M]\{\ddot{x}\} + ([K_s] + [K_x])\{x\} = K_i i + F_d$$

where  $F_d = M \mu \omega^2 e^{j\omega t}$  is the external periodic disturbance force produced by an unbalance mass attached to the rotor and  $M$  is the mass of the shaft and rotor. In the expression for  $F_d$  the rotor angular velocity is denoted by  $\omega$  while  $\mu$  is the eccentricity of the unbalance mass. In the simulations representative values for  $\mu$  have been chosen.

### REFERENCES

1. M. Dussunx.: The Industrial Applications of Active Magnetic Bearing Technology, *Proc. of the 2nd Int. Symp. on Magnetic Bearings*, Tokyo, Japan, July 1990, pp. 33.
2. K. Nonami and I. Takayuki.:  $\mu$  Synthesis of Flexible Rotor Magnetic Bearing System, *4th Inter. Symp. on Magnetic Bearings*, ETH Zurich Swaziland, August 1994, pp. 73-78.
3. Y. N. Zhuravlyov; A. Mikhail; and E. Lantto: Inverse Problems of Magnetic Bearing Dynamics, *4th Inter. Symp. on Magnetic Bearings*, ETH Zurich, August 1994, pp. 79-84.
4. M. Fujita; K. Hatake; and F. Matsumura: Loop Shaping-Based Robust Control of a Magnetic Bearing, *IEEE Control Systems Magazine*, August 1993, pp. 57-64.
5. I. Postlethwaite; Mi-Ching Tsai; and D. W. Gu: Weighting Function Selection in H-Infinity Design, *Preprint 11th IFAC World Congress*, Tallin, Estonia, August 1990, Vol. 5, pp. 104-109.
6. R. Y. Chiang and M. G. Satonov: Robust-Control Toolbox, User's Guide, *The MATH WORKS, Inc.*, 1989.
7. J. Krodkiewski and R. B. Zmood: Use of Programmed Magnetic Bearing Stiffness and Damping to Minimize Rotor Vibration, *3rd Int. Symp. on Magnetic Bearings*, Alexandria, Virginia, July 29-31, 1992.

